GOMOS Level 2 Product Quality Readme File

Field:	Contents:	Filled by:
Title	GOMOS Level 2 processor version GOMOS/6.01 Readme	SPPA Engineer
Reference	ENVI-GSOP-EOGD-QD-12-0117, issue 1.0 Date: 17 December 2012	SPPA Manager
Affected data sets	This readme file applies to all GOM_NL__2P processed with processor version IPF 6.01	SPPA Engineer
Product specification references	• Algorithm Theoretical Baseline Document (ATBD) • Product Specification: PO-RS-MDA-GS-2009, Issue 3, Revision K, 15/10/2012	SPPA Engineer

Summary — SPPA Engineer

1. GOMOS processor Version 6.01 (Level 2)

The GOMOS/ENVISAT processor version 6.01 introduces a number of upgrades that are detailed in this document and those referenced.

1.1 Processor upgrades

The following Level 2 processor upgrades have been implemented in GOMOS version 6.01:

- Accurate characterization of modeling errors in the full covariance matrix inversion: impact on error estimates and X^2
- New HRTP (High Resolution Temperature Profile) algorithm: improves the High Resolution Temperature profiles
- New coding of the error bar (logarithmic encoding of absolute error value) instead of relative error

1.1.1 Note on re-processed Version 6.01 Level 2 products

A reprocessing campaign has been performed using IPF version 6.01 of the GOMOS processor covering the period from 15th April 2002 to 8th April 2012 (end of mission). The Level 2 re-processed products are identified by the following flags reported in the MPH and in the product name:

MPH Field	***Value***
Processing stage flag	R
Processing center	FINPAC ('FIN' in the product name)
Software version	GOMOS/6.01
REF_DOC	PO-RS-MDA-GS-2009 issue 3/K

2. GOMOS Version 6.01 Level 2 products

2.1 Product data screening

To select highest quality data for scientific application, users should use the data in the GOM_NL__2P products that satisfies the following criteria:

- GEOLOCATION(30km)/SUN_ZENITH_TANGENT > 105°
- non-flagged density values: LOCAL_SPECIES_DENSITY/PCD set to "0".

Occultations from bright limb data, and to a lesser extent from twilight limb data, are of reduced quality and should be used with care.

Note that for Ozone profiles a more detailed data screening is suggested. This can be found in section 2.5.1.

2.2 Flagging and negative data

- The product flags for the retrieved quantities are processor flags, indicating if the retrieval has been successful or not.
- There is no systematic flagging of negative values of column and local densities. Negative values of line densities after spectral inversion are kept, and non-flagged negative values may be included in the vertical profiles. It is recommended to keep those data when calculating averages. Ignoring such data may introduce a risk of creating an artificial positive bias in averages of data.
- The XYZ_std fields (where XYZ is a species name) represent uncertainty estimates assuming the Gaussian error statistics. As of version IPF 6, these values represent the random error, which includes an estimate of the modeling error (mainly from incomplete scintillation correction, see Sofieva et al., 2010). Values are expressed in absolute value (cm^{-3}) of the local density and correspond to 1σ. In order to obtain the value of the standard deviation in cm^{-3} it is necessary to use a coding equation, reported in the Product Specification. This allows to convert the integer number written inside the product. The maximum value of the integer number for the error estimate is set to 6553.5.

2.3 Vertical resolution

All GOMOS occultations have the same vertical resolution, because a "target resolution" Tikhonov regularization is applied in the GOMOS inversion. The vertical resolution for different retrieved species is given in

Table 1. It is also provided in the Level 2 local densities MDS products.

Species	Vertical resolution
Ozone	2 km below 30 km; 3 km above 40 km
NO_2	4 km
NO_3	4 km
Aerosol	4 km
H_2O	2 km below 20 km; 4 km above 30 km
O_2	3 km below 30 km; 5 km above 40 km

Table 1: Target vertical resolution by retrieved species.

2.4 Altitude range of validity by product

Table 2 presents a summary of the altitude range of validity for the Level 2 products. More details for each product are given in Section 2.5.

Species	Validity/altitude range
O_3	valid at all altitudes for hot stars, in the range ~12-100 km; for cold and weak stars (mainly T < 7000K and visual magnitude > 1.9), data above 40 km should not be used
NO_2	valid between 20 km and 50 km and winter polar regions up to 65 km; data at other altitudes should be considered with caution
NO_3	valid between 25 km and 45 km, but noisy retrieved values within this altitude range; data at other altitudes should be considered with caution
Aerosols	data below 10 km and above 35 km should be considered with caution
H_2O	retrieved for 8 stars (Star_ids 1, 2, 3, 13, 14, 16, 26, 63) and up to 50 km;
O_2	valid at all altitudes; noise is observed on some profiles
HRTP	18-35 km for vertical occultations; 20-30 km for oblique occultations

Table 2: Validity assessment by altitude range and by species.

2.5 Product Characterisation

2.5.1 Ozone

The recommended screening of O_3 profiles is the following:

1. Remove profiles if:
    - GEOLOCATION(30km)/SUN_ZENITH_TANGENT < 105°
    - >40% flagged levels (LOCAL_SPECIES_DENSITY/PCD, LOCAL_SPECIES_DENSITY/QUALITY_FLAG ≠ 0)
    - vmr >20 ppmv or <-0.5 ppmv at altitudes 15-45 km
    - |vmr| > 100 ppmv and altitude 10-110 km
2. Remove specific level if
    - LOCAL_SPECIES_DENSITY/PCD ≠0
    - LOCAL_SPECIES_DENSITY/QUALITY_FLAG ≠0

	The suggested data screening removes outliers in data (see section “Outliers in ozone data below”). **It is recommended not to use ozone measurements from occultations of dim and cool stars (see section “Dim and cool star problem”)**. *<u>Known problems and features</u>* • **Tangent line density standard deviation problem in IPF 6.01** The error bars of local and tangent line densities have been changed from relative errors in % (IPF version 5.01) to absolute values (IPF version 6) without changing the field format (unsigned integer field). Therefore, a coding equation is needed (please refer to the Product Specification). Values are expressed in absolute value (cm^{-3}) of the local density and correspond to 1σ. The maximum value of the error estimate is set to 6553.5. However, it is recommended to not use the standard deviation of the tangent line density since it is **not** possible to retrieve the correct value of the **tangent line densities error**, in spite of the use of the conversion formula. Note, that the IPF 6.01 products contain correct values for the standard deviation of the **local densities**. • **Dim and cool star problem** Ozone retrieval in the mesosphere and upper stratosphere (above 40 km) is based solely on transmission values at UV wavelengths. Weak and cool stars have low S/N-ratios in this part of the spectrum. It has been found (see Kyrölä et al., 2006) that measurements (during 2003) with stars of a visual magnitude >1.9 and temperature <7000 K are not providing reliable ozone retrievals above 40 km. With the ageing of the GOMOS instrument the dark charge problem of GOMOS CCDs has increased and consequently the S/N-ratio has become lower for all stars further since 2003. By comparing statistical averages of ozone from different stars (with solar zenith angle larger than 105 deg.) 58 dim and cool stars were identified that do not support ozone retrievals above 40-50 km. Their star numbers according to the GOMOS catalogue are: **In period 2002-2004**: 3, 13, 14, 17, 26, 37, 43, 48, 50, 51, 52, 53, 54, 61, 63, 65, 75, 84, 92, 93, 94, 102, 106, 114, 116, 117, 120, 126, 137, 138, 139, 141, 148, 151, 161, 162, 165, 167, 169, 170, 171, 178; **in 2005-2008:** In addition to the above list, stars 16, 40, 101, 113, 132, 135, 142, 143, 154, 155, 157; **in 2009-2012:** In addition to lists for 2002-2008, stars 122, 134, 159, 164, 173. The ozone retrievals from these stars also show negative bias at lower altitudes (the reason for this is presently under investigation). The "bad" (dim and cool) and "good" stars on the star temperature-magnitude plane are shown in Figure 1.	

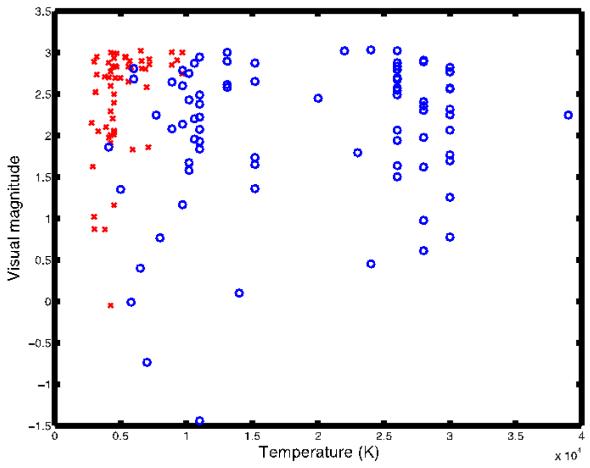

Figure 1: GOMOS stars on the star temperature-magnitude plane. The "good" stars (that have sufficient UV flux, 84 stars) at the end of the mission are shown by blue circles and the "bad" (dim and cool) stars (58) by red crosses. Note that the original weak-cool limits, visual magnitude >1.9 and temperature <7000 K, are not strict enough to describe the occurrence of bad stars.

- **Outliers in ozone data**

GOMOS ozone data have outliers, which constitute 2-4% of dark-limb data (illumination flags 0 or 3). The outlier profiles can be easily detected by visual inspection (Figure 2a).

The majority of outliers are related to the South Atlantic Anomaly (Figure 3), and they can occur also for occultations of bright stars. In other locations, outliers occur mainly for occultations of dim stars.

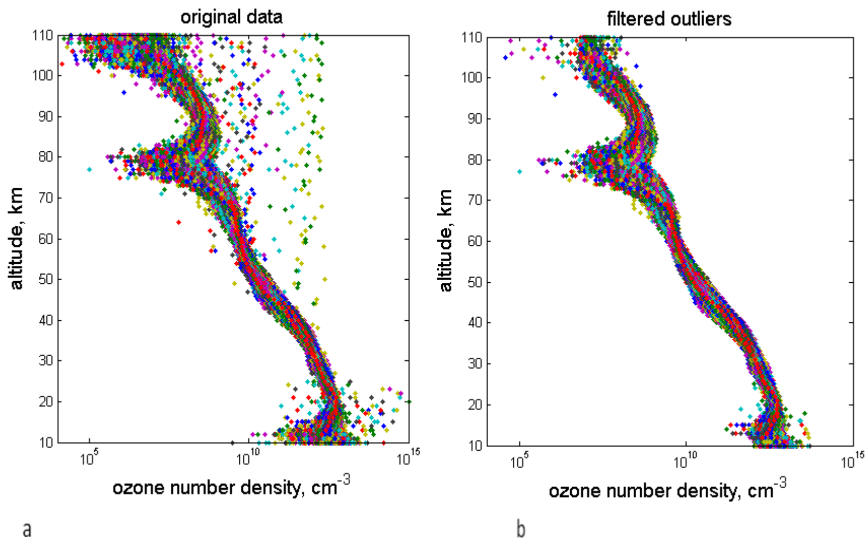

Figure 2: (a) an example of outliers in ozone data for occultations of star #7 (magnitude 0.1, T=14000K) in 2008. Colour dots correspond to individual profiles. (b) ozone data screened with the recommendation defined above.

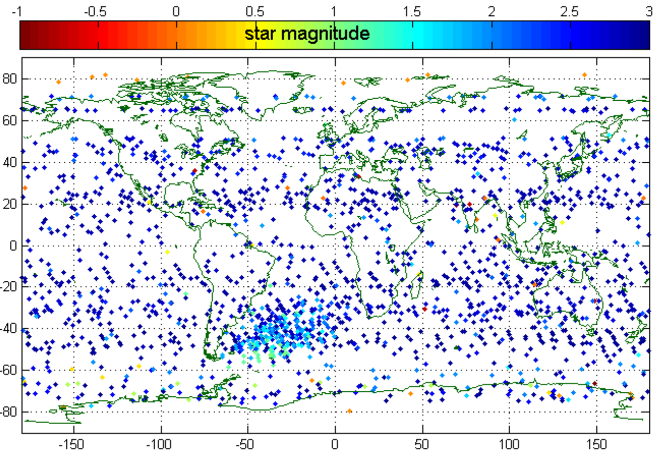

Figure 3: Locations (tangent points) of ozone outliers in 2008.

Initial Validation/Verification Results

General

The results of the systematic comparison of vertical profiles of ozone number density with NDACC lidar measurements (methodology described in Meijer et al., 2004) and with NDACC/GAW ozonesonde measurements are shown in Figure *4* and Figure 5, respectively.

The median relative difference (GOMOS-lidar) averaging results from 13 lidar stations for version 6.01, is within a few percent from 0 and shows a small negative bias for GOMOS at most altitudes. It is about -3% around 25-30 km and increases to a maximum at the top of the profile (see Figure 4).

A similar conclusion can be drawn from comparisons with data from 79 ozonesonde stations: the global median relative differences are within 3% from 15km to 32km, and mainly negative. The pole-to-pole comparison with ozonesonde measurements shows that positive biases are found in the lower stratosphere and troposphere, together with an increase of the spread. The threshold altitude of good data quality varies with latitude: from about 18-20 km in the tropics to 15 km at middle latitudes and sometimes below in polar regions.

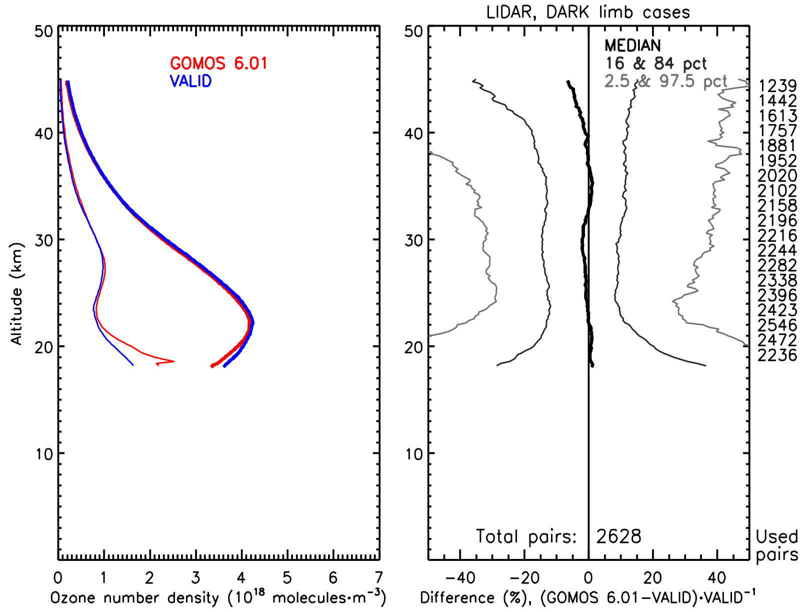

Figure 4: Left figure: Vertical profiles of the average (thick lines) and of the standard deviations (thin lines) of O_3 in number density retrieved with IPF 6.01 (red lines), and measured by ground-based lidar instruments (blue lines) between 18 and 45km. Right figure: Vertical profiles of the relative differences between O_3 in number density retrieved with IPF 6.01 and measured by ground-based lidar instruments. Lines correspond from left to right to the 2.5, 16, 50 (=median), 84 and 97.5 percentiles. Coincidence criteria between GOMOS profiles and lidar profiles are a distance within 800km and a time difference lower than 20h. Only GOMOS measurements from occultations with a solar zenith angle greater than 107º are used and a maximum error of 30% is allowed in the GOMOS and lidar data.

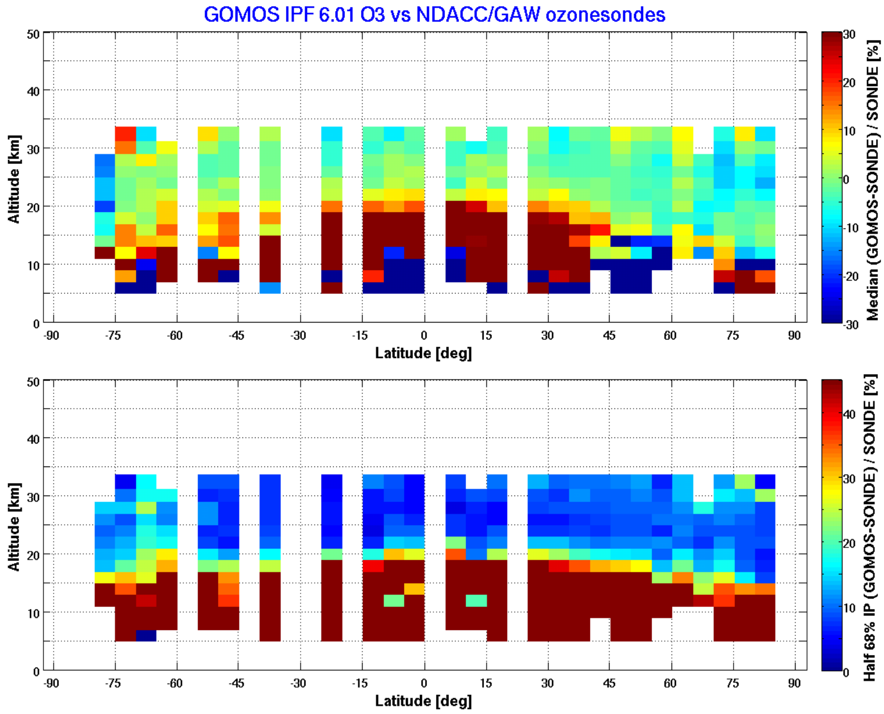

Figure 5: Latitude-altitude cross-section of the difference between ozone number densities retrieved with GOMOS IPF 6.01 and measured by the

NDACC/GAW network of ozonesondes. Top: median percentage relative difference; bottom: half 68% inter-percentile range of the relative difference (equivalent to standard deviation if the relative differences follow a normal distribution, but less sensitive to outliers than the standard deviation). Results are calculated in 5° latitude bins. GOMOS data were screened according to the recommendations in Section 2.5.1, and collocate within 500 km and up to 12h from the ozonesonde measurement.

Mid-Latitudes
The best agreement is obtained at mid-latitudes. In these regions, the median relative difference (GOMOS-validation instruments) is between -3% and +1% for altitudes between 18 km and 42 km (Van Gijsel, October 2012). Below 15 km, the comparisons to sondes indicate an increasingly positive bias.

Polar Regions
For the polar regions, a negative median difference (GOMOS-validation instruments) is found above ~15 km. Both lidar and ozonesonde comparisons indicate that the negative bias increases towards –(7-10)% at 25 km, and decreases again to 0% at 33 km. Above 33 km, the negative bias with respect to lidars increases again towards -11% at 40 km. In the UTLS and the troposphere the bias is positive, about +10% at 10 km and higher at lower altitudes. During Antarctic ozone hole conditions GOMOS ozone is 15% higher than that measured by sondes.

Tropics
In the tropics, increasing, positive (GOMOS-validation instruments) differences are found below the ozone maximum. But between 23km and 45 km, differences are again within a few percent around 0. The bias with respect to sondes is slightly positive, but remains below +3%. Lidar comparisons between 20 and 45 km show a bias between -2% and +1%.

Sensitivity to aerosol model
The concentration of ozone around the tropopause level is very sensitive to the aerosol model. For some cases, the ratio between ozone densities retrieved with two different aerosol models (2^{nd} order and 3^{rd} order polynomial for instance) is at least 1.5 below 20 km. Following intensive studies a second order polynomial was applied. This has to be considered for investigations regarding ozone at tropopause levels.

2.5.2 NO_2

The impact of the residual scintillation and of the choice of the aerosol model is reduced thanks to the DOAS inversion and regularisation.

Known problems and features

- **Tangent line density standard deviation problem in IPF 6.01**

It is recommended to not use the standard deviation of the tangent line density since it is **not** possible to retrieve the correct value of the **tangent line densities error**.
Note, that the IPF 6.01 products contain correct values for the standard deviation of the **local densities**.

Initial Validation/Verification Results

Validation studies have been based on balloon-borne stellar and moon occultation spectrometers (Renard et al., 2004) and satellite solar

occultation from HALOE (NO+NO_2 at sunset). The methodology is described in more detail in (Hauchecorne et al., 2005).
The validity range is 20 km - 50 km. In this altitude range, the random error is estimated to be about 20 %. It depends mainly on the star magnitude. The systematic error, due to the uncertainties and temperature dependence in cross-sections, is no more than 10%.

At other altitude ranges, data should be considered with caution, as the uncertainties and the temperature dependence in cross-sections may have a significant contribution to the error budget.

2.5.3 NO_3

The impact of the choice of the aerosol model is reduced thanks to the DOAS inversion.

Known problems and features

- **Tangent line density standard deviation problem in IPF 6.01**

It is recommended to not use the standard deviation of the tangent line density since it is **not** possible to retrieve the correct value of the **tangent line densities error.**
Note, that the IPF 6.01 products contain correct values for the standard deviation of the **local densities**.

Initial Validation/Verification Results

Validation studies have been based on balloon-borne stellar and moon occultation spectrometers (Renard et al., 2004). The methodology is described in more detail in (Hauchecorne et al., 2005).

The validity range is 25 km-45 km. In this altitude range, the random error is estimated to be about 30%. It depends mainly on the star magnitude although cold stars are slightly better. The systematic error, due to the uncertainties and temperature dependence in cross-sections, is no more than 15%.

At other altitude ranges, data should be considered with caution, as the uncertainties and the temperature dependence in cross-sections may have a significant contribution on the error budget.

Retrieval is still noisy within the validity range.

2.5.4 Aerosols

Aerosol spectral dependency is expressed as a 2^{nd} order polynomial. The spectral parameters given for the aerosol extinction profile are those computed during the spectral inversion and correspond to the spectral dependence of the slant aerosol optical thickness, i.e. averaged along the line-of-sight. Aerosol spectral dependence is very sensitive to residual scintillation.

Known problems and features

As the current atmosphere is extremely transparent, the capacity to retrieve individual profiles is often at the limit of the instrument sensitivity.
Very small particles are not spectrally distinguishable from Rayleigh scattering.

Polar stratospheric clouds can be detected.

Data should be considered with caution above 35 km (low aerosol extinction) and below 10 km (small signal strength). Furthermore, due to the current implementation of the spectral law, only extinction profiles at the reference wavelength of 500 nm receive Tikhonov regularization during spatial inversion. This often results in rapidly oscillating profiles at other wavelengths.
It is therefore recommended to use only 500 nm aerosol extinction profiles.

- **Local and Tangent line density standard deviation in IPF 6.01**

Note, that the IPF 6.01 products the standard deviations of the **local and tangent line densities of the Aerosol** are still stored in percentage as it was for the IPF 5.01.

Initial Validation/Verification Results

No systematic validation has been performed for aerosol extinction spectral behaviour. However, preliminary studies indicate that GOMOS aerosol extinction profiles at 500 nm are in agreement within 50 % with data from the ACE/MAESTRO mission, in the altitude range from 10 km to 35 km.

2.5.5 H_2O

Known problems and features

- **Tangent line density standard deviation problem in IPF 6.01**

It is recommended to not use the standard deviation of the tangent line density since it is **not** possible to retrieve the correct value of the **tangent line densities error.**
Note, that the IPF 6.01 products contain correct values for the standard deviation of the **local densities**.

Initial Validation/Verification Results

H_2O densities are not retrieved above 50 km.
H_2O profiles are of acceptable quality provided only by the 8 brightest stars in the near IR in dark limb (cold bright stars or very bright stars). The star numbers are: 1, 2, 3, 13, 14, 16, 26, 63. The retrieved densities from the other stars are of poor quality, related to too small SNR.

2.5.6 Neutral density

Neutral density is not retrieved with this version. The neutral density profile comes from ECMWF data completed by MSIS90 climatology above 1hPa pressure level. To avoid any confusion, products related to neutral density have been set to 0: the MDS for local density, the error bar, the vertical resolution, and the additional error. The covariance matrix terms related to neutral density have also been set to 0.

2.5.7 O_2

Known problems and features

During the period from August 25th to October 28th of each year, the second component of Star S0034 appears in the upper background band. Therefore, the occultations of this star can give degraded O_2 profiles during this period."

- **Tangent line density standard deviation problem in IPF 6.01**

It is recommended to not use the standard deviation of the tangent line density since it is **not** possible to retrieve the correct value of **the tangent line densities error.**
Note, that the IPF 6.01 products contain correct values for the standard deviation of the **local densities**.

Initial Validation/Verification Results

The relative difference between O_2 by GOMOS and O_2 by ECMWF was assessed from hundreds of dark limb occultations of star Sirius in 2003, as (O_2 GOMOS-O2 ECMWF)/ O_2 ECMWF. The O_2 from ECMWF is computed assuming an air mixing ratio of O_2 of 0.20946 constant with altitude. The mean bias is negative below 14 km, and positive between 16 and 45 km, as indicated in Table 3.

Some profiles contain outliers in the line density profiles, which propagate somewhat vertically during the vertical inversion.

Altitude range (km)	Mean bias (%)	Dispersion (%)
12 - 14 km	-3	6
14 - 16 km	0	2
16 - 30 km	+2.5	2
30 - 35 km	+5	4
35 - 40 km	+10	10
40 - 45 km	+15	20
45 – 55 km	0	30

Table 3. Mean bias and dispersion of the relative difference between GOMOS and the ECMWF taken as a reference.

2.5.8 OClO

Not retrieved in the current version of processing.

2.5.9 GAP

The GAP (GOMOS Atmospheric Profile) information is not currently provided in the geolocation ADS products. The product values are replaced by 0 and the error is set to 65535.

2.5.10 HRTP

The vertical resolution of HRTP is ~250 m. The HRTP precision mainly depends on the obliquity of the occultation. The best precision is achieved for vertical occultations. It is estimated to be about 1-2 K at altitudes between 18 km and 30 km, for vertical occultations and for close to vertical occultations.

Known problems and features

In case of a bad correlation between the photometer signals at a given altitude, the weighted mean of the time delay estimate computed using ECMWF air density and the experimental value are used. The weights are inversely proportional to uncertainties in experimental and ECMWF-model time delays. The HRTP values at this altitude are flagged (the corresponding error estimates for density and temperature are set to 6500%).

Initial Validation/Verification Results
First validation results for GOMOS version 6.01 show a very good agreement in comparison to sonde data up to 30 km (not significantly different from 0). In comparison to lidar data, the highest altitudes show an underestimation (increasing with altitude) of the temperature by GOMOS. This could be related to the upper-limit initialization used for GOMOS HRTP retrievals.

2.6 References

- **GOMOS Algorithm theoretical Basis Document**
  E. Kyrölä, L. Blanot, J. Tamminen, V. Sofieva, J. L. Bertaux, A. Hauchecorne, F. Dalaudier, D. Fussen, F. Vanhellemont, O. Fanton d'Andon, G. Barrot
  ENVISAT-GOMOS Level 1b to 2 Processing, ATBD (GOM-FMI-TN-040, issue 3.0), December 2012
- **Validation of GOMOS version 6.01 ozone profiles using ground-based lidar observations**

  Anne van Gijsel, *October 2012*

  http://earth.eo.esa.int/pcs/envisat/gomos/documentation
- **First climatology of polar mesospheric clouds from GOMOS/ENVISAT stellar occultation instrument**
  K. Pérot, A. Hauchecorne, F. Montmessin, J.-L. Bertaux, L. Blanot, F. Dalaudier, D. Fussen, and E. Kyrölä
  Atmos. Chem. Phys., 10, 2723-2735, 2010
- **GOMOS O_3, NO_2, and NO_3 observations in 2002–2008**
  E. Kyrölä, J. Tamminen, V. Sofieva, J. L. Bertaux, A. Hauchecorne, F. Dalaudier, D. Fussen, F. Vanhellemont, O. Fanton d'Andon, G. Barrot, M. Guirlet, T. Fehr, and L. Saavedra de Miguel
  Atmos. Chem. Phys., 10, 7723-7738, 2010
- **Optical extinction by upper tropospheric/stratospheric aerosols and clouds: GOMOS observations for the period 2002–2008**
  F. Vanhellemont, D. Fussen, N. Mateshvili, C. Tétard, C. Bingen, E. Dekemper, N. Loodts, E. Kyrölä, V. Sofieva, J. Tamminen, A. Hauchecorne, J.-L. Bertaux, F. Dalaudier, L. Blanot, O. Fanton d'Andon, G. Barrot, M. Guirlet, T. Fehr, and L. Saavedra de Miguel
  Atmos. Chem. Phys., 10, 7997-8009, 2010

- **Climatology and comparison of ozone from ENVISAT/GOMOS and SHADOZ/balloon-sonde observations in the southern tropics**
  N. Mze, A. Hauchecorne, H. Bencherif, F. Dalaudier, and J.-L. Bertaux
  Atmos. Chem. Phys., 10, 8025-8035, 2010
- **Response of tropical stratospheric O_3, NO_2 and NO_3 to the equatorial Quasi-Biennial Oscillation and to temperature as seen from GOMOS/ENVISAT**
  A. Hauchecorne, J. L. Bertaux, F. Dalaudier, P. Keckhut, P. Lemennais, S. Bekki, M. Marchand, J. C. Lebrun, E. Kyrölä, J. Tamminen, V. Sofieva, D. Fussen, F. Vanhellemont, O. Fanton d'Andon, G. Barrot, L. Blanot, T. Fehr, and L. Saavedra de Miguel
  Atmos. Chem. Phys., 10, 8873-8879, 2010
- **A global climatology of the mesospheric sodium layer from GOMOS data during the 2002–2008 period**
  D. Fussen, F. Vanhellemont, C. Tétard, N. Mateshvili, E. Dekemper, N. Loodts, C. Bingen, E. Kyrölä, J. Tamminen, V. Sofieva, A. Hauchecorne, F. Dalaudier, J.-L. Bertaux, G. Barrot, L. Blanot, O. Fanton d'Andon, T. Fehr, L. Saavedra de Miguel, T. Yuan, and C.-Y. She
  Atmos. Chem. Phys., 10, 9225-9236, 2010
- **GOMOS data characterisation and error estimation**
  J. Tamminen, E. Kyrölä, V. F. Sofieva, M. Laine, J.-L. Bertaux, A. Hauchecorne, F. Dalaudier, D. Fussen, F. Vanhellemont, O. Fanton-d'Andon, G. Barrot, A. Mangin, M. Guirlet, L. Blanot, T. Fehr, L. Saavedra de Miguel, and R. Fraisse
  Atmos. Chem. Phys., 10, 9505-9519, 2010
- **GOMOS ozone profile validation using ground-based and balloon sonde measurements**
  J. A. E. van Gijsel, D. P. J. Swart, J.-L. Baray, H. Bencherif, H. Claude, T. Fehr, S. Godin-Beekmann, G. H. Hansen, P. Keckhut, T. Leblanc, I. S. McDermid, Y. J. Meijer, H. Nakane, E. J. Quel, K. Stebel, W. Steinbrecht, K. B. Strawbridge, B. I. Tatarov, and E. A. Wolfram
  Atmos. Chem. Phys., 10, 10473-10488, 2010
- **Mid-latitude ozone monitoring with the GOMOS-ENVISAT experiment version 5: the noise issue**
  P. Keckhut, A. Hauchecorne, L. Blanot, K. Hocke, S. Godin-Beekmann, J.-L. Bertaux, G. Barrot, E. Kyrölä, J. A. E. van Gijsel, and A. Pazmino
  Atmos. Chem. Phys., 10, 11839-11849, 2010
- **Retrieval of atmospheric parameters from GOMOS data**
  E. Kyrölä, J. Tamminen, V. Sofieva, J. L. Bertaux, A. Hauchecorne, F. Dalaudier, D. Fussen, F. Vanhellemont, O. Fanton d'Andon, G. Barrot, M. Guirlet, A. Mangin, L. Blanot, T. Fehr, L. Saavedra de Miguel, and R. Fraisse
  Atmos. Chem. Phys., 10, 11881-11903, 2010
- **Global ozone monitoring by occultation of stars: an overview of GOMOS measurements on ENVISAT**
  J. L. Bertaux, E. Kyrölä, D. Fussen, A. Hauchecorne, F. Dalaudier, V. Sofieva, J. Tamminen, F. Vanhellemont, O. Fanton d'Andon, G. Barrot, A. Mangin, L. Blanot, J. C. Lebrun, K. Pérot, T. Fehr, L. Saavedra, G. W. Leppelmeier, and R. Fraisse
  Atmos. Chem. Phys., 10, 12091-12148, 2010

- **Retrievals from GOMOS stellar occultation measurements using characterization of modelling errors**
  V.F. Sofieva, J. Vira, E. Kyrölä, J. Tamminen, V. Kan, F. Dalaudier, A. Hauchecorne, J.-L. Bertaux, D. Fussen, F. Vanhellemont, G. Barrot, and O. Fanton d'Andon,
  Atmos. Meas. Tech., 3, 1019 – 1027, 2010.
- **Spatio-temporal observations of the tertiary ozone maximum**
  V. F. Sofieva, E. Kyrölä, P. T. Verronen, A. Seppälä, J. Tamminen, D. R. Marsh, A. K. Smith, J.-L. Bertaux, A. Hauchecorne, F. Dalaudier, D. Fussen, F. Vanhellemont, O. Fanton d'Andon, G. Barrot, M. Guirlet, T. Fehr, and L. Saavedra
  Atmos. Chem. Phys., 9, 4439-4445, 2009
- **Simultaneous measurements of OClO, NO_2 and O_3 in the Arctic polar vortex by the GOMOS instrument**
  C. Tétard, D. Fussen, C. Bingen, N. Capouillez, E. Dekemper, N. Loodts, N. Mateshvili, F. Vanhellemont, E. Kyrölä, J. Tamminen, V. Sofieva, A. Hauchecorne, F. Dalaudier, J.-L. Bertaux, O. Fanton d'Andon, G. Barrot, M. Guirlet, T. Fehr, and L.Saavedra de Miguel
  Atmos. Chem. Phys., 9, 7857-7866, 2009
- **Technical note: Scintillations of the double star α Cru observed by GOMOS/Envisat**
  V. F. Sofieva, F. Dalaudier, V. Kan, and A. S. Gurvich
  Atmos. Chem. Phys., 9, 8967-8973, 2009
- **Influence of scintillation on quality of ozone monitoring by GOMOS**
  V. F. Sofieva, V. Kan, F. Dalaudier, E. Kyrölä, J. Tamminen, J.-L. Bertaux, A. Hauchecorne, D. Fussen, and F. Vanhellemont
  Atmos. Chem. Phys., 9, 9197-9207, 2009
- **First simultaneous global measurements of nighttime stratospheric NO_2 and NO_3 observed by Global Ozone Monitoring by Occultation of Stars (GOMOS)/Envisat in 2003**
  A. Hauchecorne, J.-L Bertaux, F.Dalaudier, C.Cot, J.-C. Lebrun, S. Bekki, M.Marchand, E. Kyrölä, J. Tamminen, V. Sofieva, D. Fussen, F. Vanhellemont, O. Fanton d'Andon, G. Barrot, A. Mangin, B. Théodore, M. Guirlet, P. Snoeij, R. Koopman, L. Saavedra de Miguel, R. Fraisse, and J.-B.Renard
  J. Geophys. Res., Vol. 110, No. D18, D18301, doi: 10.1029/2004JD005711, 2005.
- **Pole-to-pole validation of Envisat GOMOS ozone profiles using data from ground-based and balloon sonde measurements**
  Y.J. Meijer, D.P.J. Swart, M. Allaart, S.B. Andersen, G. Bodeker, I. Boyd, G. Braathen, Y. Caliesi, H. Claude, V. Dorokhov, P. von der Gathen, M. Gil, S. Godin-Beekmann, F. Goutail, G. Hansen, A. Karpetchko, P. Keckhut, H.M. Kelder, R. Koelemeijer, B. Kois, R.M. Koopman, G. Kopp, J.C. Lambert, T. Leblanc, I.S. McDermid, S. Pal,H. Schets, R. Stübi, T. Suortti, G. Visconti, and M. Yela,
  J. Geophys. Res., 109, D23305, doi:10.1029/2004JD004834, 2004.
- **Validation of GOMOS vertical profiles using balloon-borne instruments and satellite data, in Proceedings of the Second Workshop on the Atmospheric Chemistry**

Validation of ENVISAT (ACVE-2)
J.B.Renard, et al.
ESA-ESRIN, Frascati, Italy, 3-7 May 2004, pp. 60.1-60.7, Eur. Space Agency, Noordwijk, Netherlands, 2004.

- **An ozone climatology based on ozone sonde and satellite measurements**
  P. J. Fortuin, H. Kelder
  J. Geophys. Res., 103, 31709-31734, 1998.

2.7 Acronyms and Abbreviations

ACE/MAESTRO	Atmospheric Chemistry Experiment/Measurement of Aerosol Extinction in the Stratosphere and Troposphere Retrieved by Occultation
ADS	Annotation Data Set
CCD	Charge Coupled Device
DOAS	Differential Optical Absorption Spectroscopy
ECMWF	European Centre for Medium-term Weather Forecast
GAW	WMO's Global Atmosphere Watch
GOMOS	Global Ozone Monitoring by Occultation of Stars
HALOE	HALogen Occultation Experiment
HRTP	High Resolution Temperature Profile
IPF	Instrument Processing Facility
LUT	Look-Up Table
MDS	Measurement Data Set
MPH	Main Product Header
MSIS90	Mass-Spectrometer-Incoherent-Scatter-1990 atmosphere model
NDACC	Network for the Detection of Atmospheric Composition Change
PCD	Product Confidence Data
PRNU	Pixel Response Non Uniformity
SATU	Star Acquisition and Tracking Unit

2.8 Acknowledgement

Input for this product quality readme file came from the GOMOS Quality Working Group, independent validation teams, and the scientific community which is responsible for the processor development.

Originator	Angelika Dehn	SPPA Engineer
Approver	Bojan Bojkov	SPPA Manager